

Beyond-mean-field theories with zero-range effective interactions. A way to handle the ultraviolet divergence

K. Moghrabi,^{1,2} M. Grasso,¹ G. Colò,³ and N. Van Giai¹

¹*Institut de Physique Nucléaire, IN2P3-CNRS, Univ. Paris-Sud, F-91406 Orsay Cedex, France*

²*Université Claude Benard Lyon 1, École Normale Supérieure de Lyon, 69364 Lyon Cedex, France*

³*Dipartimento di Fisica, Università degli Studi di Milano and INFN, Sezione di Milano, 20133 Milano, Italy*

Zero-range effective interactions are commonly used in nuclear physics and in other domains to describe many-body systems within the mean-field model. If they are used within a beyond-mean-field framework, contributions to the total energy that display an ultraviolet divergence are found. We propose a general strategy to regularize this divergence and we illustrate it in the case of the second-order corrections to the equation of state (EOS) of uniform symmetric matter. By setting a momentum cutoff Λ , we show that for every (physically meaningful) value of Λ it is possible to determine a new interaction such that the EOS with the second-order corrections reproduces the empirical EOS, with a fit of the same quality as that obtained at the mean-field level.

PACS numbers: 21.60.Jz, 21.30.-x, 21.65.Mn, 02.60.Ed

In many-body systems contact interactions are reasonable approximations to the realistic finite-range forces that can be employed in cases where the interaction range is smaller than the typical length scale represented by the interparticle distance. The main advantage of using zero-range interactions is that the equations to handle are greatly simplified. Two examples of commonly used contact interactions are the Skyrme forces which are quite popular in nuclear physics [1], and the contact interactions with coupling strengths depending on the s -wave scattering length which are employed for dilute atomic gases (see, e.g., Ref. [2]). In general, effective interactions contain parameters that must be adjusted to reproduce a given set of observables (for instance, in the nuclear case, binding energies and radii of a few selected nuclei, and bulk properties of nuclear matter). Usually this is done at the self-consistent mean-field level. When going beyond this level, it is likely that the effective interaction has to be redetermined. However, trying to discuss this issue is impossible in the case of contact interactions, since going beyond mean field, e.g., by including second-order corrections, implies dealing with contributions to the total energy which contain an ultraviolet divergence.

Many authors have studied the perturbation series for the energy of the electron gas [3–5] and of nuclear systems [6–9]. In all cases, the interaction is finite-range and no ultraviolet divergence appears. In this paper, we apply to a simple case a strategy to handle the contact interactions up to second order. We include a momentum cutoff Λ among the parameters of the interaction, and we show that for every value of Λ the other parameters can be determined in such a way that the total energy of the system with second-order contributions remains the same. This strategy, and the formulas we will show, are quite general and can be applied to different Fermi systems. For the numerical application we restrict ourselves to symmetric nuclear matter, treated with a simplified zero-range interaction.

The second-order terms that contribute to the total energy in uniform matter and diverge in the case of contact forces are shown in the lower part of Fig. 1. The divergence is caused by the integration on \mathbf{q} and is somehow unphysical since the high-momentum states are certainly outside the scale at which effective forces are to be used.

In the case of effective interactions between point-nucleons, the cutoff Λ must certainly be smaller than the momentum associated with the nucleon size, i.e., smaller than $\approx 2 \text{ fm}^{-1}$. In fact, these interactions are used to describe giant resonances or rotational bands of nuclei and consequently the scale should be even smaller, perhaps around 0.5 fm^{-1} . However, our procedure is tailored on the basic idea of renormalizable quantum-field theories: so, in principle, for any value of Λ a new set of parameters is found which leads to the same equation of state (EOS) -including the second-order contributions-. We show below that this is mathematically possible owing to the fact that the second-order correction is well-behaved as a function of the density. Thus, we imitate the QED idea that the bare electron mass and charge can be chosen for every different energy cutoff in such a way that the physical values of mass and charge are always obtained.

An ultraviolet divergence appears already at the mean-field level in the Hartree-Fock-Bogoliubov (HFB) [10] or Bogoliubov-de Gennes (BdG) [11] models when zero-range forces are employed in the pairing channel. In this case, sophisticated regularization schemes exist in which the irregular term of the pairing field is suppressed and the dependence on the energy cutoff is eliminated. These techniques are commonly adopted for example in atomic physics in BdG models [2, 12], and have been also employed in nuclear physics [13], but they cannot be directly applied to the case of interest studied in the present work.

Let us write the zero-range force as

$$V(\mathbf{r}_1, \mathbf{r}_2) = g\delta(\mathbf{r}_1 - \mathbf{r}_2). \quad (1)$$

To make contact with the Skyrme interactions [1] the

strength g is written as $t_0 + \frac{1}{6}t_3\rho^\alpha$ and this corresponds to the so-called (t_0, t_3) model that is a simplification of the usual Skyrme model where the spin-dependent, velocity-dependent and spin-orbit terms are dropped. If the Skyrme force is viewed as a G matrix (thus including ladder diagrams), the introduction of second-order contributions would in principle imply a double counting. However, our attitude is to consider as a matter of fact our interaction as phenomenological, and our framework as an effective theory where parameters are readjusted according to which diagrams are explicitly introduced.

Normalizing the single-particle wave functions within a box of volume Ω , the Hartree-Fock (HF) potential-energy contribution (upper part of Fig. 1) is equal to

$$E = d \frac{\Omega^2}{(2\pi)^6} \int_{k_1, k_2 < k_F} d^3k_1 d^3k_2 v(\mathbf{k}_1, \mathbf{k}_2, \mathbf{k}_1, \mathbf{k}_2), \quad (2)$$

where $d = (n^2 - n)/2$, n being the level degeneracy (4 in the case of symmetric nuclear matter), and $v = \frac{g}{\Omega}$. The energy per particle or EOS is obtained by adding the kinetic contribution and reads in our case

$$\frac{E}{A}(\rho) = \frac{3\hbar^2}{10m} \left(\frac{3\pi^2}{2}\rho \right)^{2/3} + \frac{3}{8}t_0\rho + \frac{1}{16}t_3\rho^{\alpha+1}. \quad (3)$$

Eq. (3) coincides with the EOS obtained with the SkP parameter set [14], in which no contribution coming from the velocity-dependent terms appears and the effective mass coincides with the bare mass. Since SkP, as all the Skyrme sets, has been fitted to reproduce within HF the basic features of the nuclear EOS, one can consider its associated energy per particle as a benchmark which must be reproduced with reasonable accuracy for every value of Λ when the second-order correction is included.

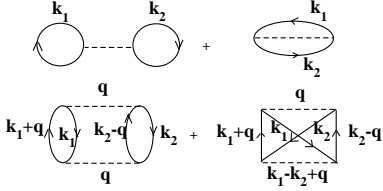


Figure 1: First- and second-order diagrams for the total energy in uniform matter. Labels refer to momentum states.

This second-order correction is given by

$$\Delta E = d \frac{\Omega^3}{(2\pi)^9} \int_{k_1, k_2 < k_F, |\mathbf{k}_1 + \mathbf{q}|, |\mathbf{k}_2 - \mathbf{q}| > k_F} d^3k_1 d^3k_2 d^3q \frac{v^2}{\epsilon_{\mathbf{k}_1} + \epsilon_{\mathbf{k}_2} - \epsilon_{\mathbf{k}_1 + \mathbf{q}} - \epsilon_{\mathbf{k}_2 - \mathbf{q}}} \equiv C \int dq v^2 G(q), \quad (4)$$

where $C = -6m\Omega^3(2\pi)^{-9}\hbar^{-2}$ for symmetric nuclear matter, and $G(q)$ reads

$$G(q) = \int_{k_1, k_2 < k_F, |\mathbf{k}_1 + \mathbf{q}|, |\mathbf{k}_2 - \mathbf{q}| > k_F} \frac{d^3k_1 d^3k_2}{q^2 + \mathbf{q} \cdot (\mathbf{k}_1 - \mathbf{k}_2)}. \quad (5)$$

Some details about the evaluation of $G(q)$ and ΔE with a zero-range force are recalled in the Appendix; finally, we write $\Delta E(\rho)/A$ as $\chi(\rho) \times I(\rho, \infty)$, with

$$\chi(\rho) \equiv -\frac{3}{4\pi^6} \frac{mk_F^7 g^2}{\hbar^2 \rho}, \quad (6)$$

$$I(\rho, \infty) \equiv \frac{1}{15} \left(\int_0^1 u du F_1(u) + \int_1^\infty u du F_2(u) \right) \quad (7)$$

where $u = q/2k_F$. When the cutoff Λ is introduced, the last integral has $\Lambda/2k_F$ as upper limit and the corresponding quantity is denoted by $I(\rho, \Lambda)$. The expressions for $F_1(u)$ and $F_2(u)$ are given in the Appendix. The analytical expression of $I(\rho, \Lambda)$ is

$$I(\rho, \Lambda) = \frac{1}{105}(43 - 46 \ln 2) - \frac{18}{35} + \frac{\Lambda}{35k_F} + \frac{11\Lambda^3}{210k_F^3} + \frac{\Lambda^5}{840k_F^5} + \frac{16 \ln 2}{35} + \left(\frac{\Lambda^5}{60k_F^5} - \frac{\Lambda^7}{1680k_F^7} \right) \ln \left(\frac{\Lambda}{k_F} \right) + \left(\frac{1}{35} - \frac{\Lambda^2}{30k_F^2} + \frac{\Lambda^4}{48k_F^4} - \frac{\Lambda^5}{120k_F^5} + \frac{\Lambda^7}{3360k_F^7} \right) \ln \left(-2 + \frac{\Lambda}{k_F} \right) - \left(\frac{1}{35} - \frac{\Lambda^2}{30k_F^2} + \frac{\Lambda^4}{48k_F^4} + \frac{\Lambda^5}{120k_F^5} - \frac{\Lambda^7}{3360k_F^7} \right) \ln \left(2 + \frac{\Lambda}{k_F} \right). \quad (8)$$

In Fig. 2(a), $E/A + \Delta E/A$ is plotted for different values of Λ and compared with the SkP mean-field values of E/A

(solid black line). The correction $\Delta E/A$ is also shown in Fig. 2(b). One observes that the second-order correction

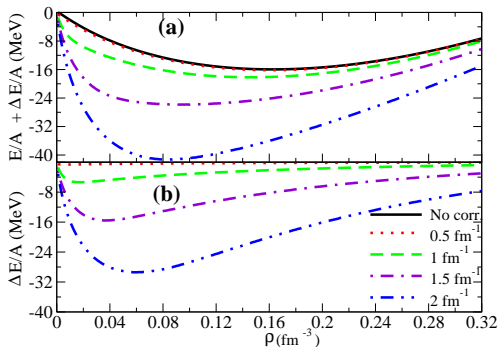


Figure 2: (Color online) (a) $E/A + \Delta E/A$ as a function of the density and for different values of the cutoff Λ . The SkP mean-field EOS (solid black line) is shown for comparison. (b) Correction $\Delta E/A$ for different values of Λ .

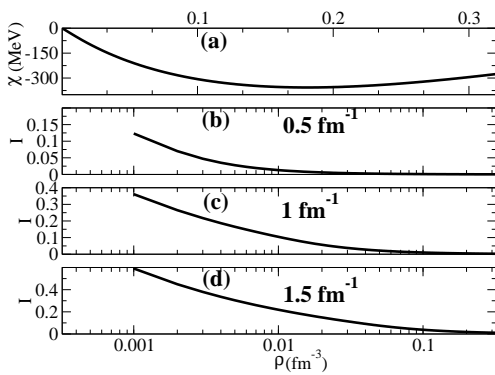


Figure 3: (a) Density-dependent χ coefficient. Other panels: the values of $I(\rho, \Lambda)$ for $\Lambda = 0.5$ (b), 1 (c) and 1.5 (d) fm^{-1} .

causes a shift of the saturation point to lower densities. The curves are calculated using the SkP parameters (cf. Table I). For $\Lambda = 1.5 \text{ fm}^{-1}$, the maximum correction is already comparable with the energy per particle at the saturation point, i.e., $\approx 15 \text{ MeV}$.

To better understand the behavior of $\Delta E/A$, we plot $\chi(\rho)$ and $I(\rho, \Lambda)$ separately in Fig. 3. The ultraviolet divergence is visible at all the values of the density, by comparing the trends in panels (b), (c) and (d). At the same time, one observes also a divergent behavior of I for $\rho \rightarrow 0$ that is dictated by the upper limit $\Lambda/(2k_F)$

One can foresee various applications to the studies of strongly correlated fermion systems in all the domains of many-body physics where zero-range forces are used and where beyond-mean-field theories are necessary for a more accurate treatment of complex correlations. In nuclear physics, models beyond mean-field theories where ultraviolet divergences appear owing to the use of a zero-

of the second integral in Eq. (7). It can be seen in the analytical expression of Eq. (8). $I(\rho, \Lambda)$ multiplies the coefficient $\chi(\rho)$ which goes to zero like k_F^4 when the density goes to zero. One may worry that for large values of Λ , the divergent behavior of the integral dominates when $\rho \rightarrow 0$, so that no regularization is possible for very low density. However, this happens for values of Λ which are physically meaningless, namely for $\Lambda \approx 250\text{-}300 \text{ fm}^{-1}$.

For each value of Λ we can perform a least square fit to determine a new parameter set SkP_Λ , such that the EOS including the second-order correction matches rather well the one obtained with the original force SkP at the mean-field level. This is our main result and it is illustrated in Fig. 4(a). The refitted parameters are listed in Table I (together with the saturation point). In Fig. 4(b) we display, for purely mathematical illustration, the refit done with the extreme value of $\Lambda = 350 \text{ fm}^{-1}$.

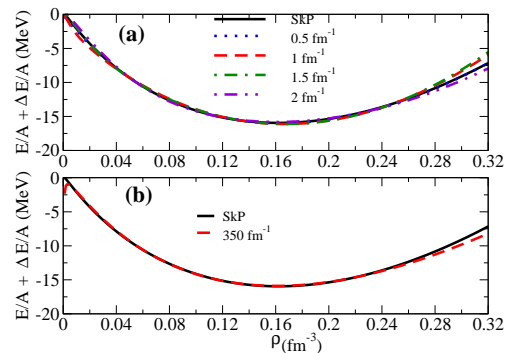


Figure 4: (Color online) (a) Second-order-corrected equations of state compared with the reference equation of state (SkP at mean-field level). (b) Extreme case of $\Lambda = 350 \text{ fm}^{-1}$.

In summary we have shown that, for any physically meaningful value of the cutoff Λ it is possible to find a contact interaction that can be used in a mean-field plus second-order corrections framework and can describe satisfactorily the empirical EOS. The quality of the fits, that can be judged from Fig. 4 and the χ^2 -values in Table I, demonstrates that the strategy we have outlined in a general fashion works, in practice, for the case of symmetric nuclear matter treated with a simplified contact force.

range interaction are: (i) models where multiparticle-multipole configurations are introduced [15], (ii) second random-phase-approximation models [16], and (iii) models that take into account the coupling between single-particle degrees of freedom and collective vibrations [17–20]. In these cases, a further development of our technique may be envisaged.

Table I: From the second line, columns 2, 3 and 4: parameter sets obtained in the fits associated with different values of the cutoff Λ compared with the original set SkP (first line). In the fifth column the χ^2/N -value (χ^2 divided by the number of fitted points) associated to each fit is shown. In columns 6 and 7 the saturation point is shown.

	t_0 (MeV fm ³)	t_3 (MeV fm ^{3+3α)}	α	χ^2/N	ρ_0 (fm ⁻³)	$E/A(\rho_0)$ (MeV)
SkP	-2931.70	18708.97	1/6		0.16	-15.95
$\Lambda = 0.5$ fm ⁻¹	-2352.900	15379.861	0.217	0.00004	0.16	-15.96
$\Lambda = 1$ fm ⁻¹	-1155.580	9435.246	0.572	0.00142	0.17	-16.11
$\Lambda = 1.5$ fm ⁻¹	-754.131	8278.251	1.011	0.00106	0.17	-16.09
$\Lambda = 2$ fm ⁻¹	-632.653	5324.848	0.886	0.00192	0.16	-15.82
$\Lambda = 350$ fm ⁻¹	-64.904	360.039	0.425	0.00042	0.16	-15.88

Acknowledgments. The authors thank Daniel Peña for useful discussions. One of the authors (G.C.) acknowledges partial support from the Italian research project (PRIN) named “Many-body theory of nuclear systems and implications on the physics of neutron stars”.

Appendix

$G(q)$ in Eq. (5) can be rewritten by expressing all wave vectors in units of k_F :

$$G(q) = k_F^4 \int_0^\infty d\alpha e^{-\alpha q^2} \int_{D_1} dk_1 e^{-\alpha \mathbf{q} \cdot \mathbf{k}_1} \int_{D_2} dk_2 e^{\alpha \mathbf{q} \cdot \mathbf{k}_2} \quad (9)$$

where the domains D_i are $D(k_i) \equiv \{k_i < 1, |\mathbf{k}_i + \mathbf{q}| > 1\}$. By introducing $y = \alpha q$, and the unit vector $\hat{\mathbf{q}} = \mathbf{q}/|q|$,

$$G(q) = \frac{k_F^4}{q} \int_0^\infty dy e^{-yq} \int_{D_1} dk_1 e^{-y \hat{\mathbf{q}} \cdot \mathbf{k}_1} \int_{D_2} dk_2 e^{y \hat{\mathbf{q}} \cdot \mathbf{k}_2} \quad (10)$$

1) First case: $q > 2$. In this case, $|\mathbf{k}_1 + \mathbf{q}| > 1$ and $|\mathbf{k}_2 - \mathbf{q}| > 1$ are satisfied when $k_1 < 1$ and $k_2 < 1$. Eq. (10) leads to

$$G_1(q) = \frac{k_F^4}{q} \int_0^\infty dy e^{-yq} \left[\frac{2\pi}{y^3} (e^y(y-1) + e^{-y}(y+1)) \right]^2 \quad (11)$$

2) Second case: $0 < q < 2$. One can apply the technique of Ref. [21], with this change of variables:

$$\int_{D(p)} dp f(p, q) = q \int_0^{2\pi} d\Phi \int_0^1 d\alpha \int_{q\alpha/2}^1 x dx f(n - \alpha q, q) \quad (12)$$

where $x = \hat{\mathbf{q}} \cdot \mathbf{n}$ and \mathbf{n} is a unit vector $\mathbf{n} = p + \alpha q$. In this case, Eq. (10) becomes

$$G_2(q) = \frac{k_F^4}{q} \int_0^\infty dy e^{-yq} \left[\frac{2\pi}{y^3} (e^{-y}(y+1) - e^{y(q-1)}(y+1) + qye^{\frac{yq}{2}}) \right]^2 \quad (13)$$

The energy correction can be written as

$$\Delta E = 4\pi C k_F^3 \left(\int_0^2 q^2 dq v^2 G_1(q) + \int_2^\infty q^2 dq v^2 G_2(q) \right) \quad (14)$$

With the change $u = q/2$ we obtain $\Delta E(\rho)/A$ as $\chi(\rho) \times I(\rho, \infty)$ [cf. Eqs. (6) and (7)], with

$$F_1(u) = \left(4 + \frac{15}{2}u - 5u^3 + \frac{3}{2}u^5 \right) \log(1+u) + \left(4 - \frac{15}{2}u + 5u^3 - \frac{3}{2}u^5 \right) \log(1-u) + 29u^2 - 3u^4 - 40u^2 \log 2; \quad (15)$$

$$F_2(u) = (4 - 20u^2 - 20u^3 + 4u^5) \log(1+u) + (-4 + 20u^2 - 20u^3 + 4u^5) \log(u-1) + 22u + 4u^3 + (40u^3 - 8u^5) \log u. \quad (16)$$

-
- [1] T.H.R. Skyrme, *Phil. Mag.* **1**, 1043 (1956); *Nucl. Phys.* **9**, 615 (1959); D. Vautherin and D.M. Brink, *Phys. Rev. C* **5**, 626 (1972).
 - [2] G. Bruun *et al.*, *Eur. Phys. J. D* **7**, 433 (1999).
 - [3] M. Gell-Mann and K.A. Brückner, *Phys. Rev.* **106**, 364 (1957).
 - [4] K. Sawada *et al.*, *Phys. Rev.* **108**, 507 (1957).
 - [5] P. Nozières and D. Pines, *Phys. Rev.* **111**, 442 (1958).
 - [6] H. Euler, *Z. Physik* **105**, 553 (1937).
 - [7] R. Huby, *Proc. Phys. Soc. (London) A* **62**, 62 (1949).
 - [8] D.J. Thouless, *Phys. Rev.* **107**, 559 (1957).
 - [9] J.S. Levinger *et al.*, *Phys. Rev.* **119**, 230 (1960).
 - [10] P. Ring and P. Schuck, *The Nuclear Many-Body Problem*, Springer-Verlag Berlin Heidelberg New York, 1980.
 - [11] P.G. de Gennes, *Superconductivity of Metals and Alloys*, Perseus Books Publishing, L.L.C. 1966.
 - [12] M. Grasso and M. Urban, *Phys. Rev. A* **68**, 033610 (2003).
 - [13] A. Bulgac and Y. Yu, *Phys. Rev. Lett.* **88**, 042504 (2002).
 - [14] J. Dobaczewski *et al.*, *Nucl. Phys. A* **422**, 103 (1984).
 - [15] L. Bonneau *et al.*, *Phys. Rev. C* **76**, 014304 (2007).
 - [16] D. Gambacurta *et al.*, *Phys. Rev. C* **81**, 054312 (2010).
 - [17] V. Bernard and N. Van Giai, *Nucl. Phys. A* **348**, 75 (1980).
 - [18] R.A. Broglia *et al.*, *Nucl. Phys. A* **752**, 345 (2005).
 - [19] G.F. Bertsch *et al.*, *Rev. Mod. Phys.* **55**, 287 (1983).
 - [20] E. Litvinova *et al.*, *Phys. Rev. C* **75**, 064308 (2007).
 - [21] D.F. DuBois, *Ann. Phys. (N.Y.)* **8**, 24 (1959).